ELSEVIER

Biophysical Chemistry 94 (2001) 275–283

Biophysical Chemistry

www.elsevier.com/locate/bpc

Substratum nanotopography and the adhesion of biological cells. Are symmetry or regularity of nanotopography important?

A.S.G. Curtis[a,*], B. Casey[b], J.O. Gallagher[a], D. Pasqui[c], M.A. Wood[a], C.D.W. Wilkinson[b]

[a]*Centre for Cell Engineering, IBLS, University of Glasgow, Joseph Black Building, Glasgow G12 8QQ, Scotland, UK*
[b]*Department of Electronics & Electrical Engineering, University of Glasgow, Glasgow, Scotland, UK*
[c]*CRISMA, Universita degli Studi di Siena, Siena, Italy*

Received 17 July 2001; received in revised form 2 November 2001; accepted 8 November 2001

Abstract

Animal cells live in environments where many of the features that surround them are on the nanoscale, for example detail on collagen molecules. Do cells react to objects of this size and if so, what features of the molecules are they responding to? Here we show, by fabricating nanometric features in silica and by casting reverse features in polycaprolactone and culturing vertebrate cells in culture upon them, that cells react in their adhesion to the features. With cliffs, adhesion is enhanced at the cliff edge, while pits or pillars in ordered arrays diminish adhesion. The results implicate ordered topography and possibly symmetry effects in the adhesion of cells. Parallel results were obtained in the adhesion of carboxylate-surfaced 2-μm-diameter particles to these surfaces. These results are in agreement with recent predictions from non-biological nanometric systems.

Keywords: Nanotopography; Adhesion; Symmetry and regularity; Cell behaviour

1. Introduction

Cells in the animal body live in an environment in which there is much nanostructure around the cells, provided by components such as collagen fibrils (topographic features reported for example in [1]) with their 66-nm repeat beading, as well as that provided by the surfaces of adjacent cells. In this paper, we report that when equivalents and simplifications of such biological nanostructures are fabricated in silica or various polymers, the cells react by marked changes in adhesion, which appear to depend on the symmetry and spacing of the nanofeatures. Not only is this of potential practical importance to the design of prostheses and devices for handling cells, but it also raises questions about the features of interfacial forces that are involved in cell adhesion.

Much work has been carried out on the reactions of cells to micrometric topography [2–6] and many cellular features, such as shape, movement, phagocytosis and gene expression, have been related to the substratum micrometric topography. Little

* Corresponding author. Tel.: +44-141-330-5147; fax: +44-141-330-3730.
E-mail address: a.curtis@bio.gla.ac.uk (A.S.G. Curtis).

0301-4622/01/$ - see front matter
PII: S0301-4622(01)00247-2

work has been carried out on the reaction of cells to disordered nanotopography (see however [7]), and consideration of reactions to regular, ordered topography is probably entirely novel. Wojciak-Stothard et al. [8] described the reaction of macrophage-like cells to anti-symmetrical steps some 100 nm deep, but did not try other patterns. These structures enhanced cell adhesion. Irregular topography seems to have little effect on adhesion as compared with planar surfaces. In preliminary experiments, we reported [9,10] very low adhesion of cells to regular arrays of nanopillars of the type shown in Fig. 1. Here, we compare the effects of several types of topography differing in regularity and sometimes in pattern symmetry.

2. Experimental

The materials used in our experiments were either fused silica surfaces patterned by electron beam lithography and dry etching in *x*, *y* and *z* directions, or silica with *z*-axis nanofeatures, such as cliffs formed by short exposure to dry etching after photolithography and random dot patterns prepared by dry etching of colloidal resists.

2.1. Methods

2.1.1. Primary fabrication: electron beam lithography

The fused silica masters for the embossing process were produced using electron beam lithography and reactive ion etching. The substrates were 25×25 mm^2 and consisted of 5×5-mm^2 areas of nanometre-scale pillars. Electron beam lithography was carried out using a Leica Microsystems Lithography EBPG 5HR beamwriter on fused silica samples, 1 mm thick. The substrates were cleaned before use by refluxing in Opticlear for 30 min prior to successive ultrasonic rinses in acetone, methanol and RO (reverse osmosis) water. A 50-nm-thick titanium layer was then deposited using an electron beam evaporator. This titanium film acts as a charge conduction layer during lithography and as an intermediate etch layer during reactive ion etching [11]. Prior to application of the resist, hexamethyldisilazane (HMDS) primer was spun onto the samples at 3000 rev./min for 1 min before baking at 80 °C. The pattern was specified using Shipley WIII DUV resist, which was applied to the substrates by spin coating at the same speed for 1 min. The samples were then soft-baked on a vacuum hotplate at 135 °C for 1 min. The electron beam lithography patterns needed to form the pillars were arrays of nanometre-scale circles. This was necessary in order to ensure that metallisation and lift-off resulted in arrays of metal pillars. The patterns were written using the beamwriter to write a large square area using a small beam spot size and a large pixel step size. For example, if a 15-nm spot is used to write a square of side 150 pm, then the square is written using a raster scan method with the distance that the spot moves between exposures being set by the pixel step size. Therefore, if the pixel step size is set to 300 nm, then the 15-nm spot exposes the resist every 300 nm, producing arrays of dots on a 300-nm pitch. The actual dot size obtained depends on the dose and the beam spot size used. Using this method, the patterns were written using doses ranging from 2 to 30 μC/cm^2 and spot sizes from 15 to 56 nm. This produced dot sizes ranging from 60 to 150 nm.

Development was carried out using Shipley CD26 developer at room temperature for 1 min followed by rinsing in RO water. A 30-nm-thick layer of NiCr (60:40) was then evaporated onto the substrates and lifted off in acetone to define the nichrome pillars on the titanium-coated fused silica. After lifting off the nichrome film, the samples were dry etched to define the pillars in titanium and then in silica. The intermediate titanium layer was etched using chlorine chemistry in an Oxford Instruments Plasmalab System 100 reactive ion etcher. $SiCl_4$ was used with a flow rate of 18 sccm at a pressure of 10 mtorr, 200 W RF power and a DC bias of -325 V. The titanium etch took 6 min at an etch rate of 8 nm/min. The nichrome pattern masks the titanium during this process, thus leaving a NiCr/Ti bilayer mask for the quartz etching. The silica was etched in CHF_3 using a Plasma Technology BP80 RIE machine with a flow rate of 30 sccm, a pressure of 23 mtorr, RF power and a DC bias of 310 V. The silica was etched for 3 min at an etch rate of 8

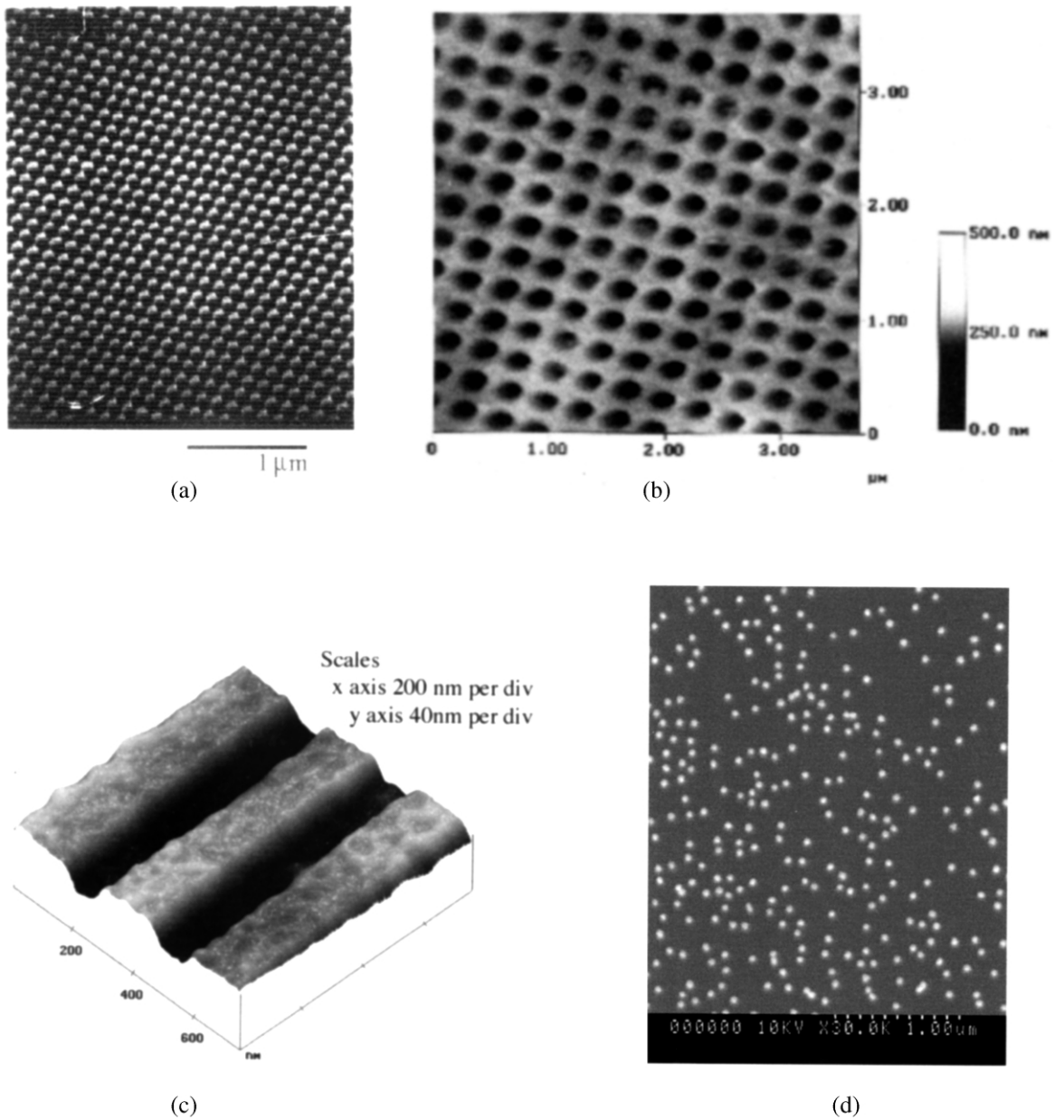

Fig. 1. AFM images of nanostructured materials. (a) In silica: array of pillars at 50-nm spacing (centre to centre), electron beam lithography and dry etch. (b) An array of pits at 250-nm spacing in polycaprolactone solvent cast from a silica master made by electron beam lithography and dry etch. Polycaprolactone cast made on a silica master using a 5% (w/v) solution of the polymer in $CHCl_3$ followed by air drying and manual stripping. (c) A cliff in silica 40 nm high made by electron beam lithography and dry etch and (d) randomly arranged dots made from gold colloid followed by dry etch (SEM). Centre-to-centre spacing of beads on average is 158 nm.

nm/min and gave a final etch depth of approximately 100 nm.

2.1.2. Replication of nanopits and pillars

The second set of structures was formed by replicating (in reverse) these patterns into polymers, such as polycaprolactone, by casting from a 5% solution in $CHCl_3$ followed by slow air-drying. The replicas were then stripped off the silica master using immersion in RO water to help debond the surfaces.

In this way, we obtained two types of *x*, *y* and *z* nanoscale patterns (pillars or pits) reproduced in silica or onto polymers and one type of *z*-scale nanofeature (cliff) in silica or the same two polymers. The pillars or pits were all of 50-nm diameter with centre-to-centre spacing of 75, 150 or 300 nm in silica.

2.1.3. Nanocliffs

The cliffs were made by forming a surface of sulfated hyaluronan and cross-linking it to the substratum by the photodynamic method described by Chen et al. [12]. Then a second layer of hyaluronan sulfate was photodynamically cross-linked over this through a mask so that 10- or 50-μm-wide stripes were formed on top of the first layer.

The stripe edges form the cliffs and AFM established their height. The pillars or pits were all of 50-nm diameter with centre-to-centre spacing of 75, 150 or 300 nm in silica or polycaprolactone. The quality of fabrication and the precise dimensions were observed by AFM (Fig. 1a,b). Control random arrays of pillars were made by colloidal lithography [13].

2.2. Atomic force microscopy (AFM) and scanning electron microscopy (SEM)

Contact-mode AFM images of the structures were made on a Nanoscope IIIa instrument.

2.3. Cells

Rat epitenon fibroblasts were grown from laboratory stocks (described by Wojciak et al. [14]) in Eagles minimal essential medium, 10% calf serum, and tryptose broth (for epitenon cells) and in Hams F10 medium, 3% fetal calf serum insulin transferrin selenite supplement (for human capillary endothelial cells) and harvested by trypsinisation at sub confluency. After washing in the same medium, the cells were made up to aliquots of 50 000 cells in 1 ml of the medium.

2.4. Measurement of adhesion and movement

A 1-ml aliquot of cell suspension was added to 2 ml of the culture medium in a Petri dish containing the silica master or polycaprolactone replica and allowed to incubate at 37 °C for 1 h. Unattached cells were removed by washing and the attached cells were counted. Time-lapse videos were recorded using phase-contrast illumination.

2.5. Detection of protein adsorption

The possibility of fibronectin adsorption from serum components of the medium was investigated by staining the structures with anti-fibronectin antibody (Dako, raised in rabbits) at 0.001% v/v for 1 h, followed by extensive washing and reaction with goat fluorescent anti-rabbit serum. After further washing the samples were examined by fluorescence microscopy using an Astrocam cooled CCD camera to detect fluorescence. This system can detect a single monolayer of fibronectin.

2.6. Fluorescent polystyrene beads

Fluorescent polystyrene beads were obtained from Molecular Probes (Eugene, OR, USA) with a diameter of 2 μm under the name Fluorospheres. Their adhesion was determined by fluorescence microscopy from images as counts of adherent particles per unit area. These beads have carboxylate surfaces. They were made up in phosphate-buffered saline, pH 7.2 (protein-free), before application to the test surfaces.

3. Results

The adhesion of two cell types (an endothelial cell line and an epitenal fibroblast line) was tested.

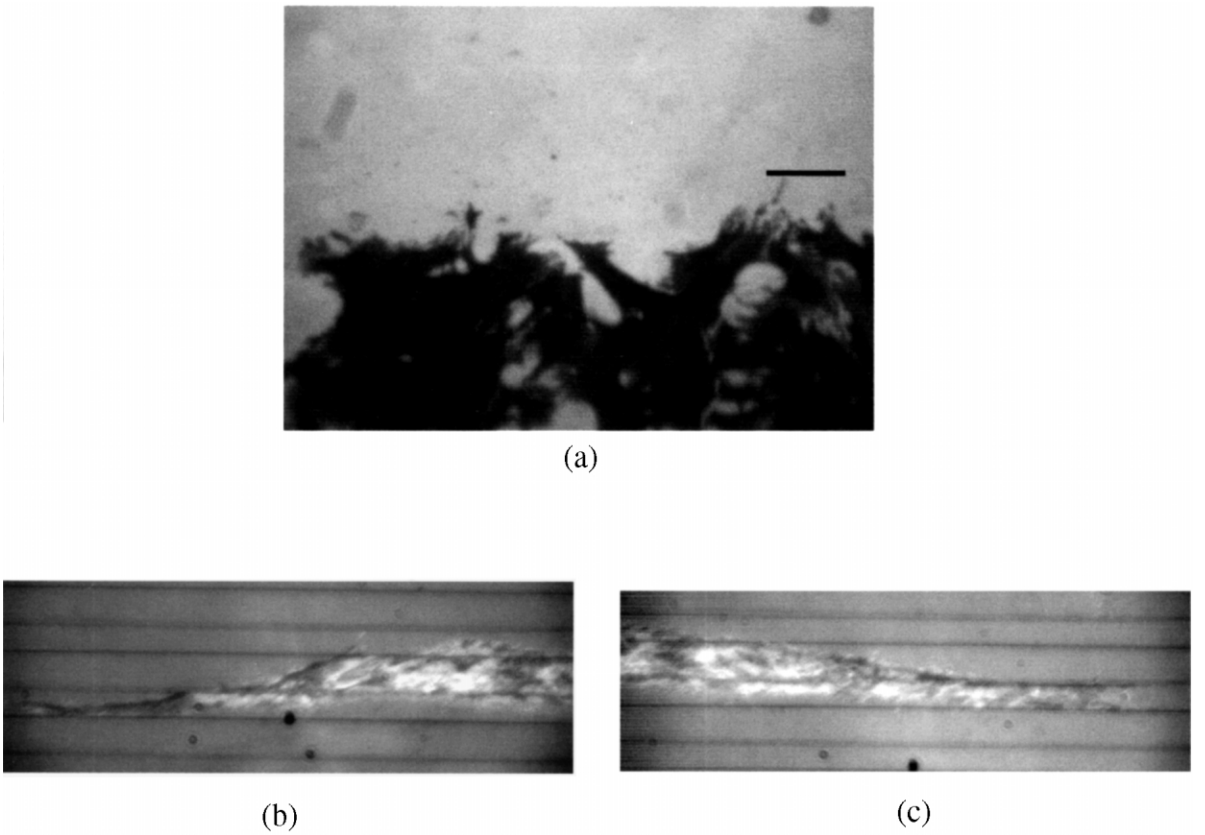

Fig. 2. (a) View of nanopit surface (shown in detail in Fig. 1b) fabricated in polycaprolactone showing very low cell attachment at 21 days compared with the control area at bottom of image. Cells stained with Coomassie blue. Scale bar, 20 μm. (b, c) Interference reflection micrographs of the contact zone of cells adhering to planar and to groove–ridge silica surfaces. This type of microscopy shows contacts where the cells are closer than approximately 10 nm as black, the same grey level as the background for 35 nm and greater separation as brighter than background. Note that the darkest parts of the image are located parallel to and very close to or superimposed on the cliffs in the substratum. Cliffs are 200 nm high and 10 μm apart, which provides an indication of the scale.

Counts of the numbers of cells attaching to a pit- or pillar-structured substrate were made and compared with the numbers attaching to the same area of planar substratum (Table 1, Figs. 1 and 2. Visualisation of nanopit areas after 21 days of cell culture showed no cell adhesion in some cases (Fig. 2a). Measuring the attachment to groove/ridge transitions as compared with the areas in between is rather more difficult, because simple observation does not give information about the contact area of the transition zone as compared with surrounding areas. In theory, the contact zone is one-dimensional. In practice, observation of the these contacts by interference reflection microscopy (Fig. 2b,c) shows that the contact is very small in area and confined to the region of transition. This in itself is reason to suggest that adhesion is very high at the groove–ridge transition. Counts of cell attachment to these regions, defined in terms of the area of the adhesive contact from interference reflection microscopy images, were made.

Counts were made of cells adhering to the nanopits in 1 h and at 5 and 20 hours, as well as

Table 1
Adhesion of cells to regular orthogonal close-packed silica nanopillars

	Rat epitenon fibroblast suspension adhering to surface (%)					
	Pillar centre-to-centre spacing (nm)				Control	
	100	150	250	300	Planar	Random dots
1 h at 37 °C[a]						
Adhesion (%)	1.2	2.9	3.7		13.9	20.2
Standard deviation	2.2	3.5	4.3		11.0	18.1
5 h						
Adhesion (%)				1.7	21.1	
Standard deviation				1.6	15.6	
20 h						
Adhesion (%)				0.76	48.3	
Standard deviation				0.9	33.2	

Counting area, 1.65 mm^2; means of counts for six areas. If 100% of the cells had adhered, the count would be 275 cells per area.

[a] This data was analysed by linear regression analysis. Standard deviation of regression coefficient 0.952, indicating a regression slope significant at $P < 0.01$.

of the proportion of the adhering cells that spread from a rounded conformation. Counts of cells adhering on a nanopillared surface were made in the same way.

Control experiments were of two types: first, the measurement of cell adhesion to planar areas adjacent to the nanostructured areas; and second, measurement of cell adhesion to a topography of random pillars (dots) (Table 1).

Table 2
Adhesion of endothelial cells to nanocliffs fabricated on sulfated hyaluronan

	Spread morphology (motile)	Rounded cells
Cliff edge	40	21
Groove bottom	0	2
Ridge top	2	19

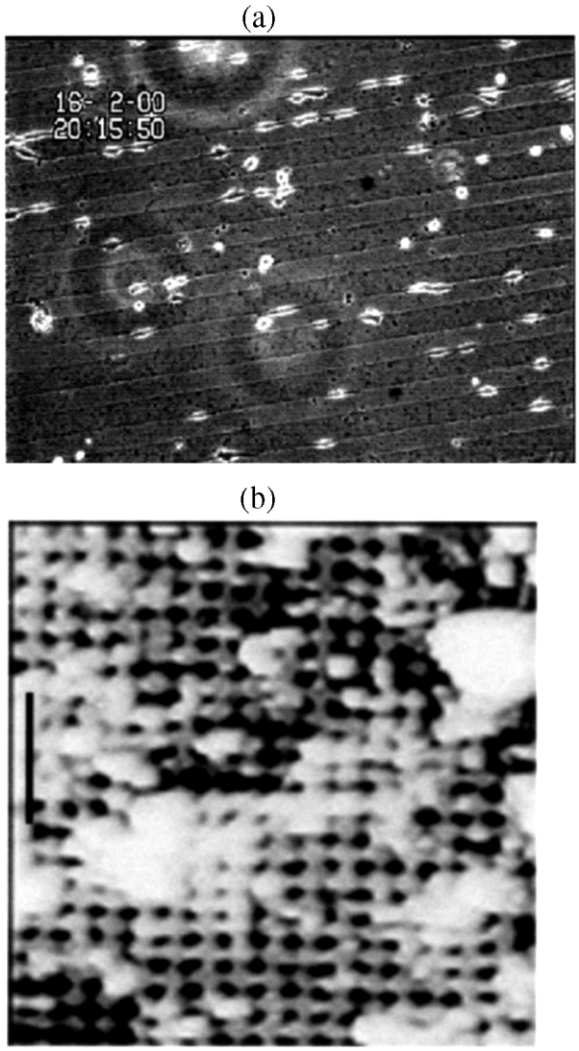

Fig. 3. Reaction of cells to nanostructured surfaces. (a) Attachment of HGTFN endothelial cells to a cliff. Optical phase-contrast view of cell attachment and alignment at the edge of a 200-nm-high cliff. (b) AFM of a polycaprolactone replica (of the type shown in Fig. 1b) after 3 weeks in culture, with pits showing zero cell attachment. The pits have been enlarged by biodegradation and are beginning to release small, pill-like pieces of polymer.

The asymmetric cliff topography enhanced cell adhesion under all conditions, except for the very smallest z-axis depths, <10 nm (Table 2, Fig. 3a). In addition, these structures enhanced cell spreading and movement along the cliff edge.

The relative contact area available to the cell (visualised by IRM as dark zones close to the ridge edges) is used to define the adhesion per unit area on nanocliffs. It is clear that these structures enhance cell spreading to a very large extent. These transition edges allowed enhanced cell movement along the transition when viewed from a time-lapse video film.

Time-lapse videos of cells on polycaprolactone pit and pillar structures (see frame from such a video in Fig. 3a) showed that cells made many attempts to attach to the structured areas, moving onto them from surrounding planar areas but failing to make permanent attachments. Frequently, a cell made two or three widely separated attachments and moved erratically, losing its attachments after some minutes. The cells often repeated these attempts to attach for periods of at least 24 h, but the lifetime of a transient adhesion at any one place was less than 1 h. When the structure was composed of regular, symmetrical pits or pillars, cell adhesion was very markedly reduced (Table 1, Fig. 2a). Surfaces bearing randomly arranged dots of the same dimensions, fabricated in the same materials and with an average spacing of 150 nm showed adhesion values close to that for planar surfaces. The comparable ordered spacing (Table 1) was very considerably less adhesive.

Little evidence for deposition of proteins was observed by AFM on such surfaces (Fig. 3b). Regular cell attachment took place on the polymer on areas clear of pattern. Immunochemical staining of these flat surfaces for fibronectin adsorption showed a low level of adsorption, which was not enhanced or depressed on adjacent structures. Table 1 also shows that as the distance between pillars is increased, adhesion increases. The random dot surfaces were little different in their adhesion from the planar surfaces. These results are consistent with the hypothesis that random patterns are not different from planar surfaces, but once ordering of the features is present, effects on adhesion are very marked.

3.1. Adhesion of carboxylate polystyrene beads

Nanopitted surfaces did not permit attachment of carboxylate beads of 2 μm in diameter. Results

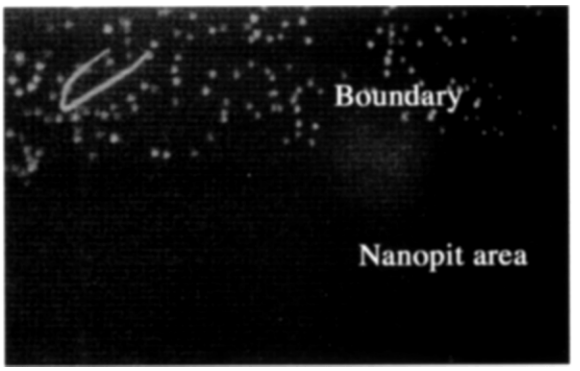

Fig. 4. Attachment of fluorescent carboxylate 2-μm-diameter beads to a nanopit surface in polycaprolactone. The medium used was protein-free saline. Note the failure of attachment over the pitted area and extra accumulation just outside the nanopitted area. The horseshoe-shaped object is a piece of cellulose lint that fell into the sample.

appeared to be similar to those obtained with cells. Note that the medium in which the particles were suspended contained no protein; compare Fig. 2a and Fig. 4.

4. Discussion

The results show that regular topography reduces cell adhesion very markedly, while discontinuities such as vertical cliffs result in high adhesion at the cliff. This discovery is, we believe, novel. The differing adhesive behaviour of the cells to ordered dots (pillars), opposed to that on random dots, suggests that substratum ordering may be important. These arrays also have symmetry. We suggest that the reaction may be to symmetry or its converse, because the cliffs are anti-symmetrical, namely the top edge is ‘convex’ and the bottom edge is ‘concave’. The cliffs, which strongly stimulate adhesion, are ordered in one dimension, but are anti-symmetrical. It is interesting to note that non-living particles of approximately the same size as cells show similar low adhesion to regular topography.

In recent months, considerable attention has been given [15–20] to the unexpected behaviour of fluids spreading on surfaces at the nanofeature level. We believe that these reports are also very relevant to the reactions of biological cells to

surfaces bearing nanotopography. Gleiche et al [16] showed non-linear behavior of interfacial forces on phospholipid strips deposited at a glass –water interface. In these and other studies, there appears to be a scale limitation to the phenomena, in that non-linear effects only appear below certain scale limits. These limits appear to lie in the 100-nm region or thereabouts and it is tempting to identify this limit with the maximum effective range of van der Waals' (dispersion) forces. We suggest that van der Waals' attractions between water 'fingers' might prevent the full wetting of a surface, but this would only occur if the forces were symmetrically balanced in an array of pillars. As the pillars become more closely packed, the Van der Waals' interactions increase, enhancing the non-wettability and this corresponds to our observations on adhesion. Conceivably, this could be further examined by making interferometic contact-angle measurements or by the use of AFM measurements. It is not yet clear how far into the pits the cells can reach, but related SEM studies by Dalby et al. [20] suggest that 100-nm features can be probed by microvilli. There is of course an imprecision in AFM measurements, especially of pits, but we gain some confidence in our measurements because of the fabrication and etch methods used to make the masters, which give alternative methods of estimating the size of pillar and pit structures.

Alternatively, on an edge with mirror-image symmetry, i.e. a cliff, forces are not balanced and this may lead to the edge becoming very wettable as the water attracts itself across the convex edge. while it does not do so across the concave edge. Rather similar but more precisely formulated approaches have been described for theoretical systems by Rascon and Parry [21].

It is interesting to note that there are a number of cellular structures similar in dimension to those we have fabricated. These are the microvilli at the surfaces of cells on which adhesions do not normally form.

The cells may be reacting directly to the topography or to some derivative feature, such as the absorption of specific proteins that aid or hinder cell adhesion. We have not detected such adsorption with fairly sensitive detection methods using fluorescent antibodies for detection of specific proteins involved in adhesion. If the protein(s) is (are) adsorbed in a way related to the symmetry of the topography of the surface, this result in itself would be powerful evidence for symmetry importance in small-range interfacial forces. On the other hand, the close similarity between adhesion of the polystyrene beads to these structures and that of the cells argues strongly that we are observing the effects of physical forces, such as interfacial ones, rather than chemical bonding. It should be noted that the beads are between 25 and 33% of the cell diameter, which places them in the same general size class.

Fig. 3 shows fairly variable reactions of cells to the same surface. This is perhaps not surprising, since the dissociated cells often retain part of their cytoskeletal organisation, and how this is oriented to the substratum when the cell first settles may well determine first reactions of the cell.

Acknowledgements

We thank the EPSRC for grant G/L83998 supporting this work, Graham Tobasnick and Bill Monaghan for technical help and Professor R. Barbucci and Dr D. Pasqui of the University of Siena for the sulfated hyaluronan.

References

[1] S.T. Boyce, D.J. Christianson, J.F. Hansbrough, Structure of a collagen-GAG dermal skin substitute optimized for cultured human epidermal keratinocytes, J. Biomed. Mater. Res. 22 (1988) 939–957.

[2] A.S.G. Curtis, M. Varde, Control of cell behaviour. Topological factors, J. Natl. Cancer Inst. 33 (1964) 15–26.

[3] G.A. Dunn, J.P. Heath, A new hypothesis of contact guidance in tissue cells, Exp. Cell Res. 101 (1976) 1–14.

[4] D.E. Ingber, D. Prusty, Z. Sun, Z.H. Betensky, N. Wang, Cell shape, cytoskeletal mechanics, and cell cycle control in angiogenesis, J. Biomech. 28 (1995) 1471–1484.

[5] B. Chehroudi, D.M. Brunette, Effects of surface topography on cell behavior, in: D.J.T. Donald, L. Wise, D.E. Altobelli, M.J. Yaszenski, J.D. Gresser, E.R. Schwartz (Eds.), Encyclopedic Handbook of Biomaterials and Bioengineering. Part S: Materials, Marcel Dekker, New York, 1995, pp. 813–842.

[6] A.S.G. Curtis, C.D.W. Wilkinson, Reactions of cells to topography, J. Biomater. Sci. 9 (1998) 1313–1329.
[7] S. Turner, L. Kam, M. Isaacson, H.G. Craighead, Cell attachment on silicon nanostructures, J. Vac. Sci. Technol. B 15 (1997) 2848–2854.
[8] B. Wojciak-Stothard, A. Curtis, W. Monaghan, K. Macdonald, C.D.W. Wilkinson, Guidance and activation of murine macrophages by nanometric-scale topography, Exp. Cell Res. 223 (1996) 426–435.
[9] C.D.W. Wilkimson, A.S.G. Curtis, Nanofabrication and its application to medicine and biology, Dev. Nanotechnol. 3 (1996) 19–31.
[10] C.D.W. Wilkinson, A.S.G. Curtis, J. Crossan, Nanofabrication in cellular engineering, J. Vac. Sci. Technol. B 16 (1998) 3132–3136.
[11] M. Elvenspoek, H. Jansen, Silicon Micromachining, Cambridge University Press, Cambridge, 1998, pp. xiv and 406.
[12] G. Chen, Y. Ito, Y. Imanishi, A. Magnani, S. Lamponi, R. Barbucci, Photoimmobilization of sulfated hyaluronic acid for antithrombogenicity, Bioconjug. Chem. 8 (1997) 730–734.
[13] P. Hanarp, D. Sutherland, J. Gold, B. Kasemo, Nanostructured model biomaterial surfaces prepared by colloidal lithography, Nanostruct. Mater. 12 (1999) 429–432.
[14] B. Wojciak, J. Crossan, A.S.G. Curtis, C.D.W. WiIkinson, Grooved substrata facilitate in vitro healing of completely divided flexor tendons, J. Mater. Sci.: Mater. Med. 6 (1995) 266–271.
[15] C. Fradin, A. Braslau, D. Luzet, et al., Reduction in the surface energy of liquid interfaces at short length scales, Nature 403 (2000) 871–874.
[16] L. Gleiche, F. Chi, H. Fuchs, Nanoscopic channel lattices with controlled anisotropic wetting, Nature 403 (2000) 173–175.
[17] A.M. Higgins, R.A.L. Jones, Anisotropic spinodal dewetting as a route to self-assembly of patterned surfaces, Nature 404 (2000) 476–478.
[18] G.P. Lopinski, D.D.M. Wayner, R.A. Wolkow, Self-directed growth of molecular nanostructures on silicon, Nature 406 (2000) 48–51.
[19] N.L. Abbot, C.B. Gorman, G.M. Whitesides, Active control of wetting using applied electrical potentials and self-assembled monolayers, Langmuir 11 (1995) 16–18.
[20] M.J. Dalby, M.O. Riehle, H. Johnstone, S. Affrossman, A.S.G. Curtis, In vitro reaction of endothelial cells to polymer demixed nano-topography, Biomaterials, in press.
[21] C. Rascon, A.O. Parry, Geometry-dominated fluid adsorption on sculpted solid substrates, Nature 407 (2000) 986–989.